Bond-stretch isomerism in strained inorganic molecules and in transition metal complexes: A revival?†

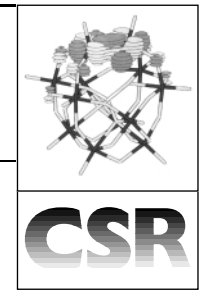

Marie-Madeleine Rohmer and Marc Bénard

Laboratoire de Chimie Quantique, UMR 7551, CNRS and Université Louis Pasteur, 4 rue Blaise Pascal F-67000. Strasbourg, France

Received 17th July 2001
First published as an Advance Article on the web 18th October 2001

A decade after Parkin's statement that 'there is presently no definitive evidence of bond-stretch isomerism in (transition metal) complexes', bond-stretch isomerism (BSI) is revisited, with special emphasis on inorganic and organometallic chemistry. It appears that the characterization of real bond-stretch *isomers*, distinct, separable and stable at room temperature, remains a very rare event. In fact, the vast majority of reports point out the case of neighboring species that were characterized with structurally distinct cores or frameworks, depending on the electronic or steric influence of peripheral substituents. In such cases, the characterization of separate energy minima on the ground state potential energy surface of an isolated molecule provides a criterion for proving the relevance of the BSI concept and also a guideline toward the synthesis of real bond-stretch isomers by means of a proper tuning of the substituents. Functionalized polyoxometalates and complexes stabilizing the $(Cr_3)^{6+}$ linear framework might provide illustrations of this strategy in the near future.

† Electronic supplementary information (ESI) available: Tables 1–6 report structural information obtained either from X-ray diffraction experiments or from *ab initio* and DFT calculations. See http://www.rsc.org/suppdata/cs/b1/b101270n/

1 Introduction

It is strange to realize that some of the most fundamental concepts in chemistry were designed and worded at a time when the intimate structure of matter was almost completely unknown. Many of them, like acido-basicity, the chemical bond or aromaticity still exist and are as essential as ever to most domains of modern chemistry, but their definition has evolved so as to incorporate the consequences of many conceptual and technological revolutions. Let us focus on the term that will be under scrutiny in the present review: isomerism. A definition given in a textbook at the end of the 19th century does not refer to the shape, or even to the constituents of molecules. Isomers were considered at the macroscopic level and defined as 'different compounds having the same centesimal composition'.[1]

The present perception of isomerism lies at the confluence of two more recent concepts: (i) the *molecular conformation*, which specifies a combination of relative atomic positions conferring on the molecule a certain stability; and (ii) the *potential energy (hyper)surface* (PES) which characterizes through its minima the various molecular conformations that could be expected for a given assembly of atoms, and defines by means of saddle points the thermodynamic pathways interconnecting them. Isomers can therefore be defined as molecular conformations corresponding to distinct minima on the PES that

Marie-Madeleine Rohmer was born in 1946 in Arras, France. After graduating from the Ecole Nationale Supérieure de Chimie de Strasbourg, she received her Doctorat d'Etat in 1975 from the Université Louis Pasteur (ULP) in Strasbourg, under the supervision of A. Veillard. After one year at Stanford University as a postdoc, working on heme models with Dr G.-H. Loew, she went back to the ULP where she has now a position of Directeur de Recherche at the Centre National de la Recherche Scientifique (CNRS). Her major research field is ab initio *and DFT quantum chemistry, with a special interest in large transition metal systems and related computational problems. During the last few years, she has focused on the electronic structure and topology of polymetallic nanostructures.*

Marc Bénard was born in 1945 in Le Havre, France. He graduated in 1969 from the Université de Provence (Marseilles, France) after completing a thesis supervised by Professor André Julg. In 1966, he joined the CNRS, where he is presently Director of Research. After a postdoctoral stay at Munich, Germany, as a Humboldt Fellow, he joined the Laboratoire de Chimie Quantique at the Université Louis Pasteur (Strasbourg, France) created in the late sixties by Alain Veillard. He became interested in the computational problems that occur in the ab initio *calculations of large molecules, in the nature of the chemical bond in transition metal complexes, and in the associated distributions of electron density. Those fields of interest then slowly evolved toward the treatment of high-nuclearity complexes, cages and clusters by means of* ab initio *and DFT methodologies.*

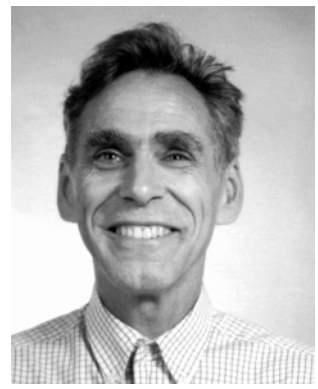

 DOI: 10.1039/b101270n

are separated by an energy barrier high enough to impede immediate interconversion at room temperature. In practice, a barrier of 30 kcal mol^{-1} or more is necessary to keep the isomers separated for a few minutes in ambient conditions.[2] The molecular conformations separated by lower energy barriers are rather termed *conformers*. They are not separable under ambient conditions, but could be observed and characterized at lower temperature. In fact, this border of 30 kcal mol^{-1} makes a link with the old definition of isomerism based on macroscopic observation.[1] It is clear, however, that the range of energy barriers, directly related to time scales for interconversion, is continuous from 0 to >100 kcal mol^{-1} and that the terms *isomers* and *conformers* basically refer to chemical species of the same nature.[2]

Accurate knowledge of molecular conformations in the solid state is presently available by means of X-ray crystallography, provided that the structure is not disordered. There are frequent cases where structural changes are observed that should be assigned to differences in the molecular environment. Such changes can be important. A typical example is provided by the complex Re(*cis*-Cl_2)(NCMe)(NO)-*trans*-$(PMe_3)_2$, which crystallizes in the space group $P2_1/a$ with 44 molecules in the asymmetric unit, interconnected through a remarkably dense and low-symmetry hydrogen bonding network.[3] All individual rhenium complexes display the same ligand organization, but the Re–N_{NO} and the Re–N_{NCMe} distances may vary by as much as 0.10 or 0.12 Å, respectively, between different molecules of the asymmetric unit.[3] Does this represent a case of *bond-stretch isomerism*, as discussed by the authors? It is clear that the answer should be no, because the structural discrepancies cannot be assigned to a specific collection of atoms. On the one hand, DFT calculations carried out on one isolated Re(*cis*-Cl_2)(NCMe)(NO)-*trans*-$(PMe_3)_2$ molecule yielded a single energy minimum, thus proving that the structural variability is indeed an environmental effect.[3] On the other hand, modelling the whole asymmetric unit as a single supramolecular compound—should it be technically possible—would also lead to a unique energy minimum for a supersystem reproducing the structural variability observed in the unit cell. This example shows that the observation of structural differences may not be sufficient to imply isomerism. The complete characterization of isomers (or conformers) should in principle require the assignment of the structurally distinct atomic assemblies to *separate minima* on a calculated—or experimentally determined—PES.

With the counter example of Re(Cl_2)(NCMe)(NO)$(PMe_3)_2$, we have introduced the term *bond-stretch isomers*. This term was coined by Stohrer and Hoffmann to particularize the case where isomers do not differ in the three-dimensional arrangement of atoms.[4] Later on, Parkin reworded this concept and defined bond-stretch isomerism (BSI) as 'the unusual phenomenon whereby molecules differ only in the length of one or more bonds'.[5] The word 'unusual' is important: the concept of BSI was first developed as a *gedanken experiment* and the early attempts to trap real bond-stretch isomers either failed or were eventually rejected as crystallographic artefacts.[5] Still presently, very few compounds that are presented as bond-stretch isomers referring to Parkin's definition have been separately characterized at room or even at low temperature *and* been shown to satisfy the criterion of the double energy minimum. However, the concept of BSI violates in no way the laws of thermodynamics and hence, the production of bond-stretch isomers should be accessible to chemical engineering. This challenge therefore contributes a large part to the present appeal of BSI and even incomplete characterizations and controversial reports show that the matter is topical and provide clues toward future and—hopefully—successful investigations. The present paper is intended to review some recent work concerning molecules on which both structural information and energy profiles are available, at least in part. For most of the compounds, mainly inorganic or organometallic, that will be under scrutiny, it is not possible yet to decide with certainty whether they truly and unambiguously comply with Parkin's definition, but each of them illustrates an aspect of BSI or defines a route that could eventually lead to bond-stretch isomers. These various aspects, and some illustrative examples, include the following.

Could isomers, or conformers, exist for a diatomic molecule? The case of Cr_2.

Competition between various stabilizing factors in small strained inorganic molecules such as the heavier homologs of bicyclo[1.1.0]butane, or isostructural, phosphorus-containing systems.

Through-ring bonding in edge-sharing dimers of octahedral complexes: metal–metal bond, or ligand–ligand bond?

'Geometric isomerism' based on the mobility of three Ru–Ru bonds in the mixed-valence, cubane like complex $[Cp_2Cp^*_2Ru_4S_4]^{2+}$.

The intramolecular redox system: coupling a dimetallic fragment with a single M–M bond to an electron reservoir. The example of γ-$[SiW_{12}O_{40}]^{6-}$ and related systems.

The three-electron, three-center bond in M_3(dipyridylamide)$_4Cl_2$ (M = Co, Cr): what is the origin of the structural variability in the organometallic equivalents of the allyl radical?

2 The chromium dimer: a benchmark for theory and experiment

An archetypal example of BSI, and possibly the only one to comply *stricto sensu* with the definition, would be to characterize a diatomic species exhibiting two distinct equilibrium positions. The conjecture seems counterintuitive: either an unsupported bond exists, and can be assigned a definite bond length and a specific bond energy, or it is broken. Weak van der Waals associations likely to occur at long distance will not be taken into consideration. It appears, however, that some transition metal dimers in the middle of the period are very close to, or even could possibly display, two minima on their potential energy curve, both assignable to electronic coupling. Let us focus on the case of the chromium dimer, which has been most extensively studied both experimentally[6] and theoretically.[7] The ground state of atomic Cr is $^7S_3$, corresponding to a $(3d)^5(4s)^1$ valence electron configuration. A simplistic scheme would therefore involve consideration of the complete spin pairing of two ground state atoms, which yields a $^1\Sigma_g^+$ chromium dimer with a closed shell $(3d\sigma_g)^2(3d\pi_u)^4(3d\delta_g)^4(4s\sigma_g)^2$ valence electron configuration: this is the famous 'sextuple bond'. The observed Cr–Cr distance in the chromium dimer is indeed the shortest known metal–metal bond: 1.6788 Å, to be compared with 2.5 Å in metallic chromium.[6] Rotationally resolved studies of the intense A ← X band near 460 nm confirmed that the ground state is a singlet obtained from multiple spin coupling. Other experimental studies, as well as early theoretical investigations, revealed, however, that the bonding is much more complex than suggested by the simple picture of the sextuple bond. The observed dissociation energy, 1.44 ± 0.05 eV, is actually smaller than that of the singly bonded Cu_2 (2.078 eV) and the ground state potential appears exceedingly sensitive to the influence of the rare gas matrix. The 3d–3d bonding was eventually analyzed in terms of a delicate balance between (1) the *spin pairing* (or covalent bonding) scheme, which corresponds to the single, closed-shell determinant characteristic of the sextuple bond and implies a zero spin density in the vicinity of each metal atom; and (2) the opposite picture of *antiferromagnetic coupling*, which can be described in the first approximation as leaving the two metal atoms in a high-spin

atomic state, with up-spin population on atom A and down-spin population on atom B.[8]

Furthermore, it was pointed out very early that the optimal bonding regions are quite different for the 3d and for the 4s orbitals. Calculations carried out by Goodgame and Goddard on Cr_2 using a modified generalized valence bond (MGVB) method were first to predict a double-well potential, dominated by d–d bonds at short distance, and by the s–s bond and d–d antiferromagnetic coupling at long distance.[9] On the experimental side, Moskovits *et al*. reported that when matrix isolated Cr_2 molecules are pumped with radiation corresponding to the $^1\Sigma_g^+ \longrightarrow {}^1\Sigma_u^+$ absorption, a new absorption appears, belonging to a metastable species of Cr_2.[10] The new state was interpreted as being either a member of the ground state manifold of states with high spin multiplicity, or alternatively the long bond form of ground state Cr_2 predicted by Goodgame and Goddard. Moskovits *et al*. noted that according to this interpretation, the production of the metastable species was not unlike an 'isomerization'.[10]

More recently, photoelectron spectra of Cr_2^- were reported by Casey and Leopold, showing two series of vibrationally resolved transitions to the ground state of neutral Cr_2.[6] A least-squares fit of the observed levels resulted in the potential energy curve reproduced in Fig. 1, with a plateau in the region

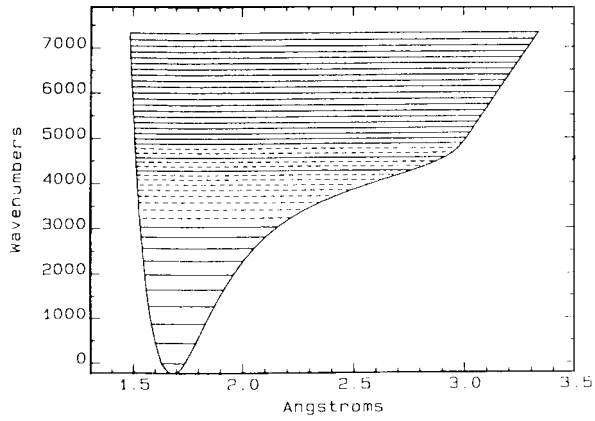

Fig. 1 Fit of the 30 observed vibrational levels of Cr_2 according to the Rydberg–Klein–Rees (RKR) method to give the $^1\Sigma_g^+$ ground state potential energy curve. Solid lines indicate observed levels, and dashed lines indicate calculated levels that were not observed. Reproduced from the work of S. M. Casey and D. G. Leopold[6] with permission.

comprised between 2.2 and 3.0 Å.[6] A comparison between the fitted potential with the double-well potential predicted by Goodgame and Goddard (Fig. 2) points out the quantitative

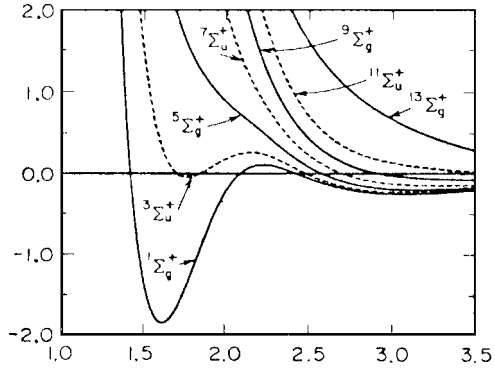

Fig. 2 Potential energy curves calculated using an MGVB method by M. M. Goodgame and W. A. Goddard, III[9] for the singlet ground state of Cr_2 and for all spin states dissociating to the ground state atoms. Energies in eV, distances in Å. Reproduced from ref. 9 with permission.

inadequacies of the theoretical model: a calculated potential too steep and harmonic in the lower energy region, and energy values too high in the region of the barrier and of the outer well. However, Casey and Leopold concluded that a qualitative agreement indeed existed between the general bonding picture proposed by Goodgame and Goddard and the experimental data: both can be interpreted in terms of a rapid loss of bonding between the compact 3d orbitals beyond the equilibrium position, partially offset as the atoms separate by increased intra-atomic exchange stabilization as well as by improved 4s–4s bonding. They finally noted that the fit of the spectral data reproduced in Fig. 1 was not devoid of uncertainty, especially in the region of the shelf (3040–4880 cm^{-1}) where the vibrational data are missing. They did not exclude the fact that the true potential actually displays a shallow minimum in this region, which leaves open the possible existence of bond-stretch conformers.

The modelling of the ground state energy profile of Cr_2 combines most of the difficulties that can be encountered in the quantum theoretical treatment of a small molecule. It is only in recent years that the experimental characteristics of the equilibrium position (R_e, D_e, ω_e) could be reproduced with reasonable accuracy by means of *ab initio* calculations.[7,11,12] The potential energy curves obtained from these calculations are in good qualitative accord with the experimental profile of Casey and Leopold and agree with the presence of a more or less flat shelf in the region of 4s–4s bonding. Fig. 3 reproduces two of these calculated curves, compared to the fit of Fig. 1.

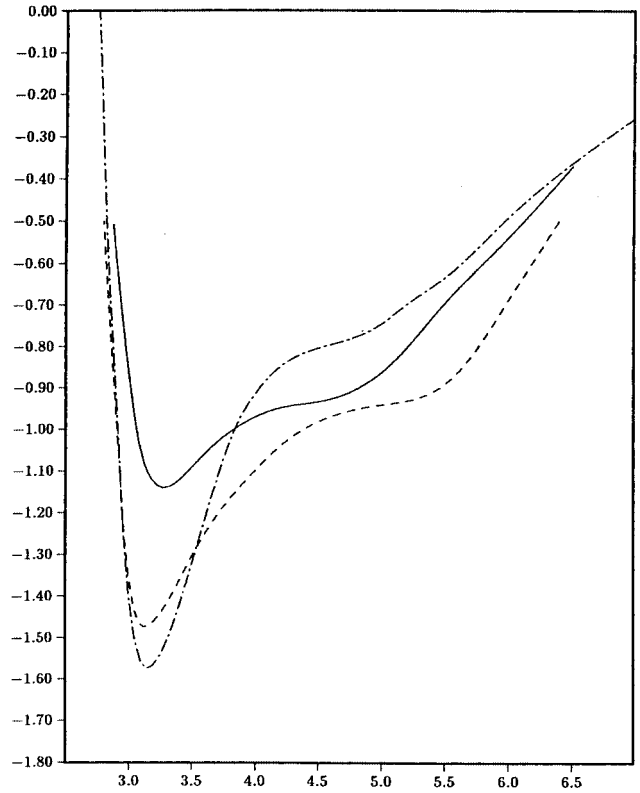

Fig. 3 The $^1\Sigma_g^+$ ground state PES of Cr_2 calculated by Stoll and Werner[11] using the multireference average coupled pair functional (MRACPF) method (solid line) and compared to CASPT2 calculations (dash–dotted line) and to the experimental curve of Fig. 1 (dashed line). Energies in eV, distances in bohrs. Reproduced from ref. 11 with permission.

The energy profile of Cr_2 has also been modeled by means of density functional theory (DFT). The recent calculations reported by Edgecombe and Becke address more specifically the problem of the double-well potential.[13] The correct balance between covalent bonding and antiferromagnetic coupling of the 3d electrons is ensured by using a spin-unrestricted, broken-symmetry formalism, completed by an approximate projection on the pure singlet spin state. The bonding energies and the potential curves appear extremely dependent upon the ex-

change-correlation functional. The most realistic results (R_e = 1.59 Å; D_e = 1.38 eV) are obtained with the hybrid functional B3P86, including some proportion of the Hartree–Fock-like exchange. But the most important outcome is that the potential energy curve displays a second, shallow minimum at 2.40 Å, with an outer well depth of 0.03 eV and a bond energy of 1.14 eV (Fig. 4). These results seem compatible with the experimental profile, given the uncertainty in the shelf region.[13]

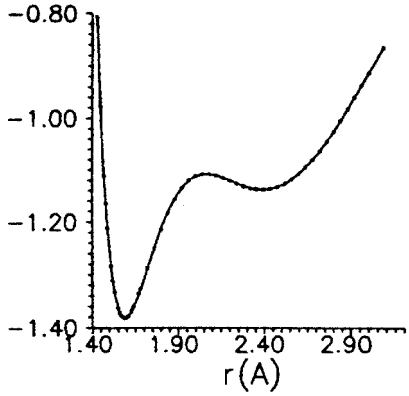

Fig. 4 The $^1\Sigma_g^+$ ground state PES of Cr_2 calculated by Edgecombe and Becke[13] using a spin-projected, broken-symmetry DFT approach with the hybrid B3P86 functional for exchange correlation. Energies in eV, distances in Å. Reproduced from ref. 13 with permission.

To summarize, no conclusive answer can yet be given to the question of bond-stretch isomerism in the chromium dimer. An outer minimum of the ground-state energy curve, if it exists at all, should anyhow be extremely shallow and the corresponding isomer rather short-lived and difficult to trap and to characterize. The dimeric species isoelectronic to Cr_2, dimolybdenum and ditungsten, are expected to display the same trends. Goodgame and Goddard noted some similarity between the ground state energy profiles of Cr_2 and Mo_2 calculated with the MGVB method, even though an inflection, but no second minimum was obtained in the long-bond region.[9] To our knowledge, no further study, either experimental or theoretical, can presently shed more light on the behavior of these species.

3 Bond-stretch isomerism in strained systems

3.1 Bond stretching in [1.1.1]propellane, bicyclo[1.1.0]butane, and their heavier analogs

The original idea of Stohrer and Hoffmann in introducing bond-stretch isomerism was based upon the specific spatial conformation and electronic behavior of a strained hydrocarbon, the tricyclo[2.2.2.0]octane or [2.2.2]propellane.[4] This molecule, as other [*m.n.p*]propellanes, has a symmetry plane Σ perpendicular to the central axis 1–4 (Scheme 1). The hybrid orbitals pointing at the axial carbons can overlap in a combination symmetric with respect to the Σ plane (S orbital) so as to generate a transannular C–C bond.

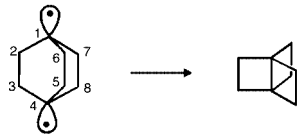

Scheme 1 Reproduced from ref. 4 with permission.

This S orbital has an antibonding counterpart A, antisymmetric with respect to Σ, which should—in principle—remain unoccupied and higher than S for all values of the transannular distance. However, in the specific case of [2.2.2]propellane, an interaction known as through-bond coupling occurs between orbital A and the high-lying σ* orbitals of the three outermost C–C bonds 2–3, 5–6 and 7–8, resulting in a stabilization of A. Because of the through-bond interactions, a crossing occurs between A and S so that orbital A becomes the LUMO when the transannular distance is larger than 2.25 Å and gives rise to a diradical form. The orbital crossing makes the interconversion between the diradical and the tricyclic form symmetry-forbidden and should generate isomers, that is, equilibrium conformations separated by an energy barrier (Fig. 5).[4]

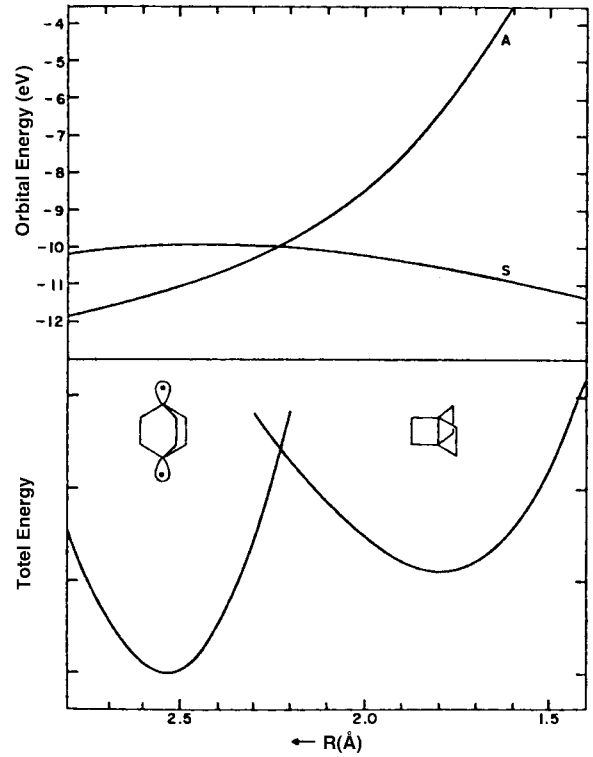

Fig. 5 HOMO and LUMO energies (top) and total energies (bottom) as a function of the transannular C–C distance *R* in [2.2.2]propellane, from extended Hückel calculations by Stohrer and Hoffmann.[4] The energy scale interval in the bottom part is 0.5 eV between the ticks. Reproduced from ref. 4 with permission.

It was also pointed out however that ring opening to 1,4-dimethylenecyclohexane from the outer minimum was an allowed process which should occur without a barrier (Scheme 2). Such a rearrangement into a dimethylenecycloalkane should

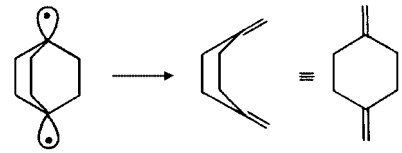

Scheme 2 Reproduced from ref. 4 with permission.

therefore prevent the formation of stable bond-stretch isomers. However, the formation of a monocyclic species is a forbidden process for the other members of the propellane series. Unfortunately, the stabilization of the antisymmetric orbital by means of through-bond interactions is not favored in tricyclic species having at least one cycle with an odd number of atoms and most of the carbon [*m.n.p*]propellanes with small *m*, *n* and *p* values were expected to display short transannular bonds on the basis of extended Hückel calculations.[4] This prediction was later confirmed by the synthesis of [1.1.1]propellane and the determination of an internal bond length of 1.596 ± 0.005 Å by

means of gas-phase electron-diffraction data. Calculations later carried out on [1.1.1]- and [2.2.2]propellane at the *ab initio* level and including a minimal amount of electron correlation[14] seemed to confirm the analysis proposed by Stohrer and Hoffmann. However, the most conclusive statement concerning the rearrangements that could occur in [2.2.2]propellane was recently issued by Davidson,[14] from the comparative analysis of a series of methodological approaches, all including electron correlation. The results ascertain that [2.2.2]propellane exists as a separate energy minimum and has a substantial barrier to opening to the bicyclic diradical or to the dimethylenecyclohexane. The open diradical form is lower in energy than propellane, but occupies only a shallow well if it exists at all, before opening to the much more stable dimethylenecyclohexane.[14]

Replacing carbon by its heavier homologues in small propellanes and other strained species does not modify the orbital sequence and no dramatic change in the electronic structure can be expected as a function of the transannular distance. However, the heavier atoms have a lower tendancy to form s–p hybrid orbitals with high p character and tend to maintain in their compounds their ns^2np^2 electronic valence configuration. This property favors the formation of compounds with 90° bond angles, while the three-membered rings become disadvantageous since they require the overlap of hybrids with high p character.[15] The balance between the stabilization due to bond formation and the increased strain associated with three-membered rings becomes less favorable for short transannular bonds and bond-stretched structures were predicted by theory for [1.1.1]propellanes of silicon, germanium and tin. The X-ray characterization of a derivative of pentastanna[1.1.1]propellane has confirmed the stretching of the central bond, with a transannular distance of 3.367 Å compared to an average value of 2.86 Å for the six peripheral bonds.[15]

The same competition between ring strain and bond formation is at the origin of some of the rare cases of bond-stretch isomerism that could be unambiguously characterized by the calculation of a double-well potential. It concerns the silicon and germanium analogues of bicyclo[1.1.0]butane, Si_4H_6 and Ge_4H_6, and was also shown to occur in mixed bicyclic systems composed of silicon and carbon. In all cases and at all levels of calculation, the bond-stretched form was found to be lower in energy (Table S1, ESI).[15,16] A multiconfiguration treatment, which seems most appropriate for this problem, gave an energy difference of 17 kcal mol^{-1} in favor of the long bond form of Si_4H_6.[17] Note that both equilibrium conformations are on the same singlet potential energy surface and that each structure retains major bonding character for the central bond. The energy barriers are extremely low: a barrier of only 1.2 kcal mol^{-1} was obtained from generalized valence bond calculations on Si_4H_6 (Table S1, ESI).[18] Such conditions are not favorable to the observation of separate isomers and it seemed obvious that an X-ray characterization should confirm the greater stability of the long bond form. Rather surprisingly, the experimental structure of a derivative of bicyclo[1.1.0]tetrasilane with bulky substituents, $(Si\text{-}tBu)_2[Si\text{-}(2,6\text{-}Et_2C_6H_3)_2]_2$ was found to closely reproduce the *short-bonded* structure predicted for the less stable isomer (Table S1, ESI).[17] This result nicely illustrates the ambiguity of bond-stretch isomerism in systems other than diatomics. Even though the internal Si–Si bond length clearly represents the reaction coordinate of the isomerization process, other geometrical transformations occur that are likely to selectively modify the nonbonding interactions between the substituents.

In Si_4H_6, the interflap angle between the three-membered ring moieties increases from ~120° to ~140° as the internal Si–Si bond elongates. The flattening of the bond-stretched M_4H_6 structure is still more pronounced with M = Sn (144°) and Pb (152°).[15] This opening of the structure is combined with a dramatic change in the orientation of the hydrogens at the bridgehead positions: the Si–Si–H angles decrease from ~140° to ~90° so that the bridgehead hydrogens closely approach one another (Fig. 6; Table S1, ESI). Replacing hydrogens at these positions by methyl substituents (Table S1) or still more conspicuously by *t*-Bu groups will obviously favor the short-bonded conformation.

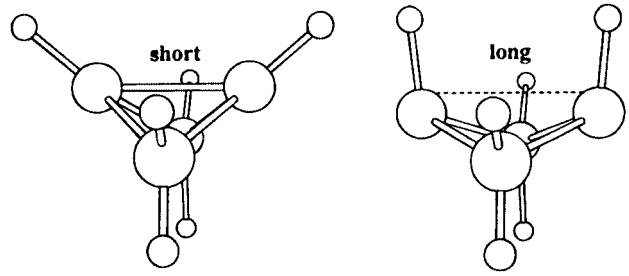

Fig. 6 Schematic representation of the two isomers of the M_4R_6 compounds (M = Si, Ge, Sn, Pb; R = H, alkyl). Reproduced from the review article by S. Nagase[15] with permission.

Electropositive substituents like SiH_3 have been calculated to make the s–p hybridization less unfavorable in polyhedral compounds of silicon and heavier homologs and therefore to significantly reduce the skeletal strain. This property, combined with the steric repulsion between bulky groups in the long bond form has been taken advantage of for the synthesis of $[Si\text{-}Si(t\text{-}Bu_3)]_4$, the first silicon equivalent of tetrahedrane.[15] Calculations carried out on Si_4R_4 with R = SiH_3 predicted the bond-stretch isomer of Fig. 7 to be more stable by 10.4 kcal mol^{-1}. Fine tuning of the R substituent could possibly allow both isomers to be detected or even separated at low temperature, depending on the interconversion barrier.[15]

Observation of structural variability involving the short-bonded and the bond-stretched forms of butterfly M_4 species was recently reported for the $(Ge_4)^{6-}$ anion.[19] This anion polymerizes with Ba^{2+} counterions as a Zintl phase which possesses a phase transition at 630 K. In the structure observed at room temperature, half of the $(Ge_4)^{6-}$ anions exist as isolated butterfly units with a short central Ge–Ge bond (2.58 Å), similar in length to the peripheral bonds (2.57 Å). The remaining anions have been condensed in the form of cross-linked polymers of butterfly units chained together by an intermolecular linkage (d_{Ge-Ge} = 2.874 Å) somewhat longer than the peripheral, single Ge–Ge bonds (2.60 Å). The structure of the individual $(Ge_4)^{6-}$ anion *in the polymer chain* is that of a bond-stretched butterfly with a central Ge–Ge distance elongated to 3.274 Å.[19]

3.2 Competition between bond formation and π delocalization: the two conformations of diphosphabicyclo[1.1.0]butane[20]

A case of BSI involving a diphosphabicyclo[1.1.0]butane system has been recently reported and substantiated by the X-ray structures of the two isomers and by *ab initio* calculations on the long-bonded form.[20] It seems however that π delocalization and aromaticity rather than ring strain are the key factors in the competition between the short-bonded and the bond-stretched isomers. The four-membered system exhibiting this photochemically induced ring closure is of the form $(ArP)_2CRCH$, with Ar = 2,4,6-$tBu_3C_6H_2$ and R = $SiMe_3$. Like the well documented case of N_2S_2, the isoelectronic cyclic compounds $(AR)_2B_2$ (A = C; B = O, S) or $(AR)_2(BR')_2$ (A = C; B = N, P) have been expected to benefit from the delocalization of a 6π electron system. The first such system to be reported and characterized was $(ArP)_2(CCl)_2$, which displayed a square planar P_2C_2 ring with a significant pyramidalization at both the phosphorus and the carbon atoms (Table S1, ESI). *ab initio* MCSCF calculations on the $(PH)_2(CH)_2$ model system predicted the ground state to be a singlet with a strong diradicaloid

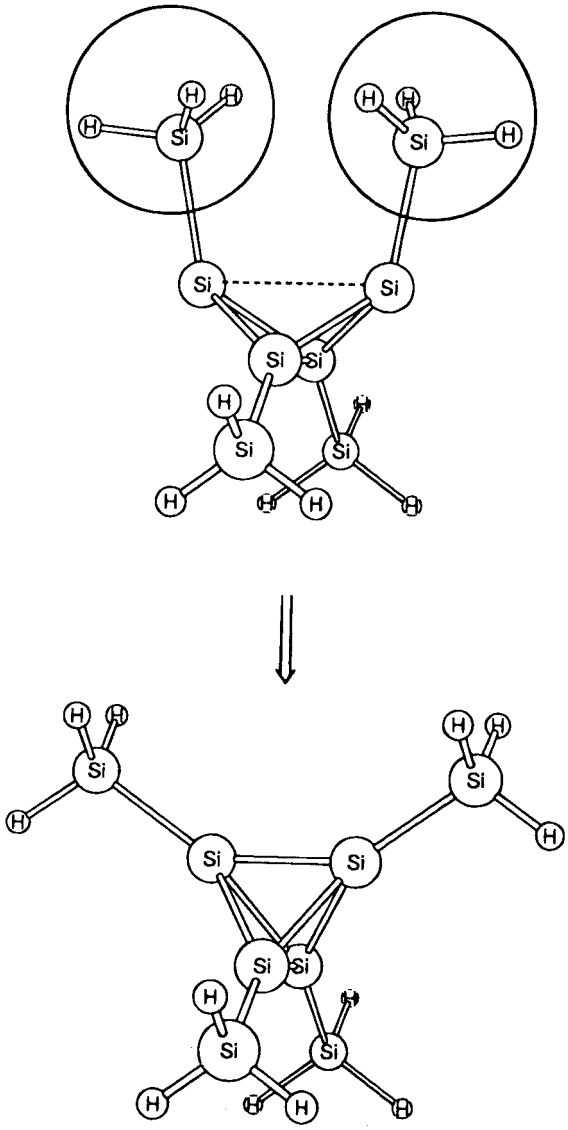

Fig. 7 Schematic representation of the two isomers expected from calculations carried out on silyl substituted tetrasilatetrahedrane Si_4R_4 (R = SiH_3 or $Si(alkyl)_3$). Reproduced from the review article by S. Nagase[15] with permission.

character at the carbon atoms and an optimized geometry in close agreement with the X-ray structure. However, no isomer with a transannular C–C bond was obtained for this compound. Such an isomer was obtained very recently[20] with a closely related, but nonsymmetric species in which the Cl substituents on carbon had been replaced by hydrogen on one side and by $SiMe_3$ on the other (Fig. 8).

As for $(ArP)_2(CCl)_2$, the 6π electron diradicaloid form was isolated in the form of a red crystalline solid and characterized as a square planar species with short P–C bonds (1.73 Å) indicative of an important delocalization in the π system (Fig. 8a). This compound is thermally stable and is not affected by brief heating to 150 °C. However, irradiation induces a rapid conversion into the diphosphabicyclo[1.1.0]butane, a yellow solid whose X-ray structure displays a transannular C–C single bond (1.516 Å), a folding of the P_2C_2 ring (117.3°) and a stretching of the P–C bonds to typical single bond values (1.84 Å) due to the loss of π delocalization (Fig. 8b). No theoretical study has yet been reported on these two compounds, but there is little doubt—if the singlet ground state of the planar species can be confirmed—that they represent the first product for which two bond-stretch isomers, strictly corresponding to Parkin's definition and in keeping with Stohrer and Hoffmann's considerations, could be separated and independently characterized at room temperature.

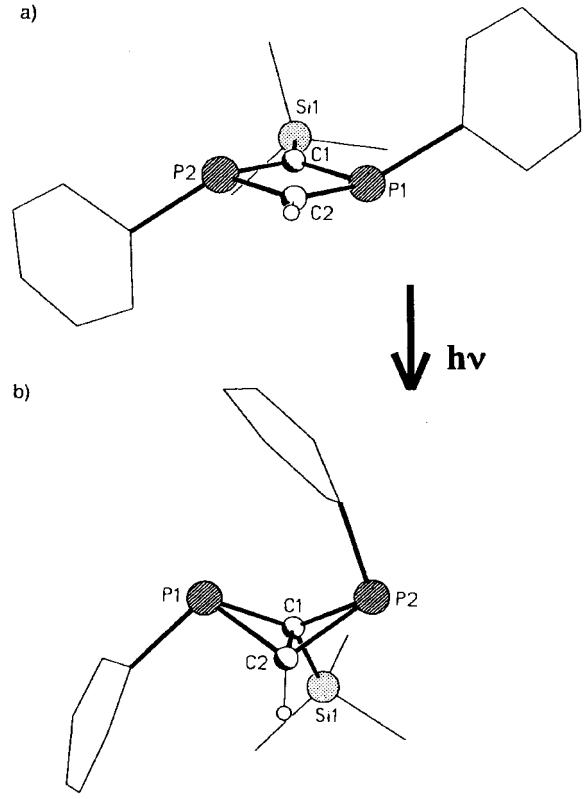

Fig. 8 Simplified representations of the crystal structures obtained by Niecke *et al.*[20] for the two isomers of $[(Mes^*P)_2\ CHCSiMe_3]$: a) 1,3-diphosphacyclobutane-2,4-diyl form; b) 1,3-diphosphabicyclo-[1.1.0]butane form. Reproduced from ref. 20 with permission.

3.3 Competition between delocalization patterns in polycyclic hydrocarbons[21,22]

A different type of strain resides in the contiguousness in some polycyclic hydrocarbons of aromatic and antiaromatic systems. The archetypal model for such a valence isomerism is benzocyclobutene, in which cyclobutadiene is combined with benzene in an overall 8π electron system. The possible competition between the two π systems **1a** and **1b** (Scheme 3)

1a **1b**

Scheme 3 Reproduced from ref. 21 with permission.

was investigated by means of MP2/3-21G calculations and two energy minima were characterized and assigned to a symmetry-forbidden interconversion process between the π-based HOMO and LUMO.[21]

The quinoid form **1b** is however destabilized by almost 50 kcal mol^{-1} and the local minimum found at the MP2 level could not be confirmed by CASSCF calculations.[21] The X-ray structure of a derivative of benzocyclobutene shows a double bond between C7 and C8 and a slightly distorted benzene ring, in agreement with the conformation of Scheme 3, left. Calculations, however, suggested that a more balanced competition could occur between valence isomers **2a** and **2b** of benzo[1,2:4,5]dicyclobutene (Scheme 4). Rather surprisingly, the synthesis and characterization of 3,6-di-*tert*-butyl-7,8,9,10-tetraphenylbenzo[1,2:4,5]dicyclobutene yielded a compound with D_{2h} symmetry, as for **2a**, but retaining neither the aromatic character of the central ring, nor the double-bond picture of the outermost C–C linkages, C7–C8 and C9–C10 (**2c**).[22]

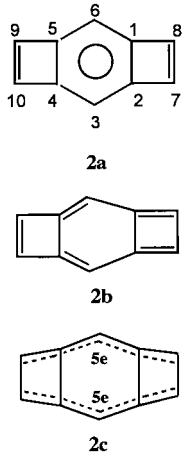

Scheme 4

Both conformations **2a** and **2c** were calculated as distinct and almost isoergonic minima at the DFT-B3LYP/6-31G* and *ab initio* MP2/6-31G* levels of theory (Table S2, ESI). Even though Boese *et al*.[22] represented isomers **2a** and **2c** with similar bonding patterns, namely an aromatic ring with two double C–C bonds, an analysis of the calculated and observed bond lengths in **2c** rather suggests a system composed of two delocalized pentyl radicals connected through four C–C single bonds C7–C8, C9–C10 (R4); C1–C2 and C4–C5 (R2). The vinyl substitution at the cyclobutene rings extends and stabilizes the two conjugated subsystems and strengthens the single bond character of R4. The order of magnitude of the energy barrier separating isomers **2a** and **2b** and the possibility of an interconversion process are currently being investigated.[22]

4 Isomerism based on intramolecular redox processes involving metal–metal bonds

Various examples of fluxional behavior and in some cases the characterization of distinct structures in transition metal chemistry can be assigned to intramolecular redox processes implying electron transfers from metal to ligand, or from metal to metal, or from a dimetallic fragment to an electron reservoir. The changes in the molecular structure associated with such redox processes are quite relevant to bond-stretch isomerism.

4.1 Ring deformation in edge-sharing dimers of transition metal complexes[23–25]

The structural variability in the M_2X_2 rings formed between late transition metals and bridging ligands in compounds of general formula $[M_2(\mu\text{-}XR_m)_2(L_n)_2]$ (m = 0–2) offers interesting potential for bond-stretch isomerism. These complexes may appear in any of the three forms represented in Scheme 5.

The structural behavior of the M_2X_2 rings has been independently analyzed by the groups of Alvarez[23] and Mealli.[24] In this review, we will mainly follow the argument of

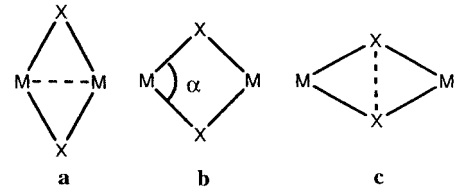

Scheme 5 Reproduced from ref. 25 with permission.

Alvarez who rationalizes the formation or breaking of transannular bonds by introducing the concept of *framework electron count* (FEC). The FEC represents the number of electrons involved in bonding between the metals and the bridging ligands. The counting convention assumes that each ML_n fragment is electronically saturated with respect to the 16- or to the 18-electron rule, and able to act as a four-electron acceptor toward the bridging ligands. All the electrons participating in framework bonding are therefore provided by the bridging atoms, together with any extra electrons required by the molecular charge. An FEC of 8 will be associated in general with the square ring of Scheme 5b, whereas an FEC of 6 or 4 will induce through-ring bonding, either metal–metal, or ligand–ligand.[23]

Intramolecular redox processes between the metals and the bridging ligands will modify the FEC and therefore induce a structural change in the M_2X_2 ring. A typical case studied by Alvarez concerns the reduction of the metal atoms and the concomitant formation of a ligand–ligand bond (Scheme 6).[23] The orbital diagram of Fig. 9 summarizes the reorganization of the four metal–ligand bonding orbitals and their two lowest antibonding counterparts as the X–X distance diminishes so as to form a through-ring bond. The ligand weight decreases and eventually vanishes in the combinations with X–X antibonding character, either σ* (b_{3u}), or π* (b_{2g}). The metal population increases accordingly, *i.e.* the metal is reduced; the $(X)_2$ fragment tends toward a conformation with an X═X double bond, or toward an intermediate status that can be interpreted as a transannular single bond. According to the convention given above, the electrons involved in X–X bonding are withdrawn from the FEC, which decreases from 8 to 6 or 4 (Scheme 6). Structural data obtained for dichalcogen bridged Pd and Pt complexes either from experiment or from theory show that both the square planar and the X–X bonding conformations can occur, depending on the metal, on the bridging ligand (S, Se or Te) and on the L–M–L angle, which can be constrained to be small by using chelating diphosphines.[23]

Calculations on the model complexes $Pd_2(\mu\text{-}S)_2(PH_3)_4$ and $Pd_2(\mu\text{-}S)_2$(diphosphinoethane)$_2$ show a minimum for a conformation with an S–S single bond, whereas another minimum was found with a long S–S distance and a butterfly bending of the Pd_2S_2 ring. Theoretical *and experimental* evidence for an isomerism based on the reversible cleavage of an intracyclic ligand bond was found in the family of the synthetic analogues of oxyhemocyanin $Cu_2(\mu\text{-}O)_2(L)_2$, where L represents a tridentate ligand such as the anion of tris(3,5-dialkylpyrazolyl)borate (^{R}TPB), or 1,4,7-trialkyl-1,4,7-triazacyclononane (^{R}TACN). An equilibrium between the $[Cu_2(\mu\text{-}\eta^2\text{:}\eta^2O_2)]^{2+}$ and $[Cu_2(\mu\text{-}O)_2]^{2+}$ conformations of $Cu_2(\mu\text{-}O)_2(^{i\text{-}Pr}TACN)_2$ was

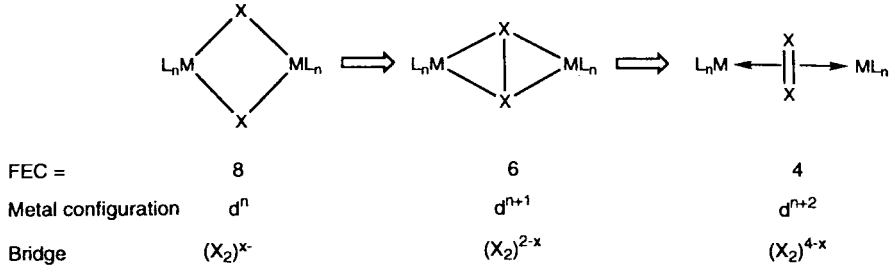

Scheme 6 Reproduced from ref. 23 with permission.

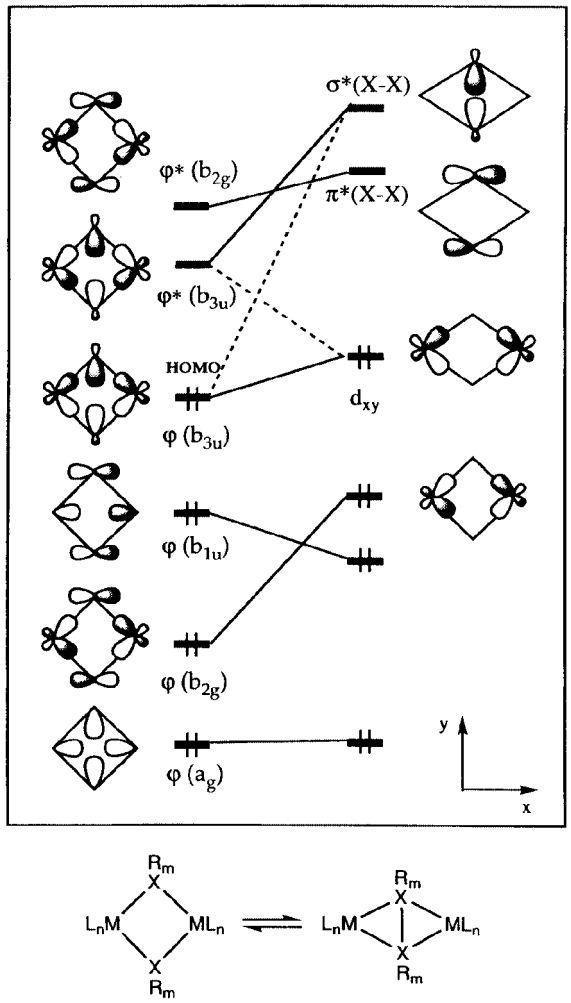

Fig. 9 Simplified orbital correlation diagram for an M_2X_2 ring into its two isomeric forms without and with a through-ring X–X bond. Reproduced from ref. 23 with permission.

suggested, and authenticated by the X-ray structure of the bis-μ-oxo form of the closely related compound $Cu_2(\mu\text{-}O)_2(^{i\text{-}Bn}TACN)_2$ (Bn = 1,4,7-tribenzyl-1,4,7-triazacyclononane).[26] The Cu···Cu, Cu–O and O···O distances are 2.794, 1.81 and 2.287 Å, respectively, in the observed crystal of $Cu_2(\mu\text{-}O)_2(^{i\text{-}Bn}TACN)_2$, to be compared with 3.560, 1.92 and 1.41 Å for the characterized peroxo form of another synthetic analog of oxyhemocyanin. The reversible cleavage of the O–O bond in $Cu_2(\mu\text{-}O)_2(^{i\text{-}Pr}TACN)_2$ was further substantiated on the basis of kinetic and spectroscopic arguments.[26] Mealli and Orlandini have recently proposed a simple explanation of the dichotomy of the $Cu_2(\mu\text{-}O)_2(L_3)_2$ species.[24b] Indeed, these authors noted that the vanishing of the O–O transannular bond was accompanied by a rearrangement of the terminal ML_3 units leading to a planar $Cu_2(\mu\text{-}O)_2(L_2)_2$ complex with no O–O bond and only loosely attached to the third potential ligand of the macrocycle.[24b]

Another possibility to induce BSI in M_2X_2 rings exhibiting a framework electron count lower than 8 could be the tuning of an equilibrium between forms **a** and **c** of Scheme 5, characterized by a metal–metal or a ligand–ligand bond, respectively.[25] At variance with the discussion related to the reductive cleavage of an X–X bond, such a process does not involve any change of the FEC. In edge-sharing dimers of octahedral complexes of the type $[M_2(\mu\text{-}XR_2)_2L_8]$, the four orbital combinations stabilized by the metal–ligand interactions ($1a_g$, $1b_{1u}$, $1b_{2g}$, $1b_{3u}$, see Fig. 9) are topped by a group of 6 t_{2g}-like metal orbital combinations, so that the complex can accommodate up to 20 'ring electrons'. When the FEC is equal to 6, the conformation exhibiting a metal–metal bond occurs as a single minimum with all systems for which the number of ring electrons (NRE) remains lower than 18. When NRE = 18, a conflict occurs between orbital $1b_{3u}$, with M–M bonding and X–X antibonding character (Fig. 9) and orbital $2b_{1u}$ belonging to the t_{2g} set, which acquires a strong M–M antibonding character as the metal–metal distance increases. The energy of these two orbitals is strongly dependent upon the structure of the M_2X_2 ring (Fig. 10): a short M–M distance will favor the occupancy of orbital $1b_{3u}$, whereas the formation of an X–X bond will be stabilized through the occupancy of orbital $2b_{1u}$.[25]

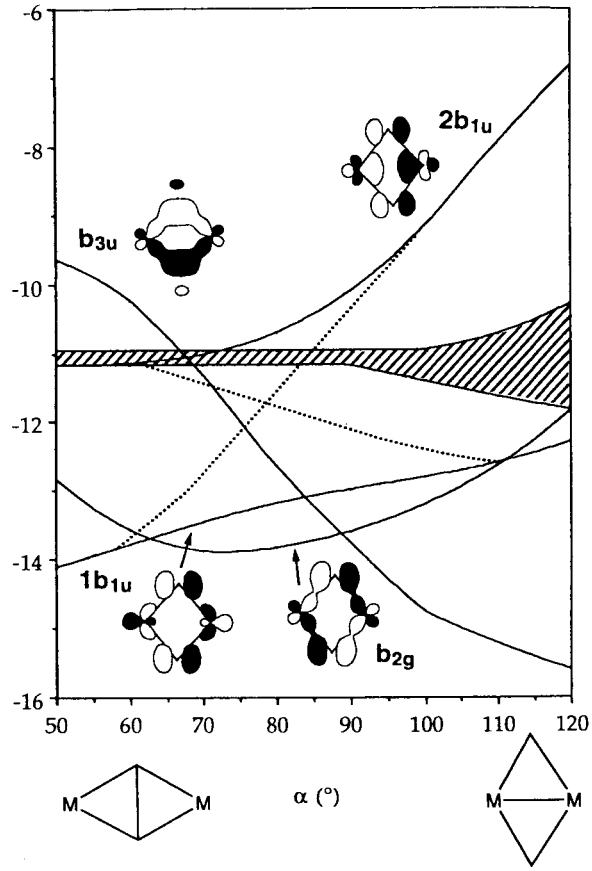

Fig. 10 $[M_2(\mu\text{-}XR_2)_2L_8]$: Walsh diagram illustrating the dependence of the frontier orbitals $1b_{3u}$ and $2b_{1u}$ upon the ring distortion measured by the XMX angle, α. From extended Hückel calculations by Palacios *et al.*[25] Energies in eV. Reproduced from ref. 25 with permission.

Density functional calculations on the lowest singlet and triplet states of $[Cr_2(\mu\text{-}PH_2)_2(CO)_8]$ (NRE = 18, FEC = 6) confirm for each spin state the existence of a double minimum corresponding to conformations **a** and **c** of Scheme 5. The main geometrical features of the optimized structures are displayed in Table S3 (ESI). The complex $[Mn_2(\mu\text{-}SiPh_2)_2(CO)_8]$, characterized by the same ring electronic configuration (NRE = 18, FEC = 6) was structurally characterized by a metal–metal bond. However, the isoelectronic complex $[Mn_2(\mu\text{-}SiH_2)_2(CO)_8]$ was calculated not to be isostructural: the singlet ground state corresponds to conformation **c** with an Si–Si bond. Adding two electrons to these complexes increases both the NRE and the FEC to 20 and 8 electrons, respectively. It has been shown above that an FEC of 8 is not compatible with a transannular bond. In accordance with this rule, the two dianions are calculated to have a single energy minimum corresponding to a square (**b**) conformation.[25]

4.2 'Geometric isomerism' in cubane-like M_4S_4 clusters[27,28]

Fluxional behavior in a cubane-like structure involving a reorganization of the metal–metal bonding network was first

demonstrated by Kubas and Vergamini in 1981.[29] The synthesis of a series of iron–sulfur clusters containing the S_2 ligand was reported. On the basis of the X-ray structures known for the closely related systems $Cp_4Fe_4S_4$ and $Cp_4Fe_4S_6$, it was assumed that the $Cp_4Fe_4S_5$ (**3**) cluster and its oxidized counterparts adopt a cubane-like Fe_4S_5 structure in which one chalcogenic vertex is replaced by the disulfur moiety (Scheme 7).[29]

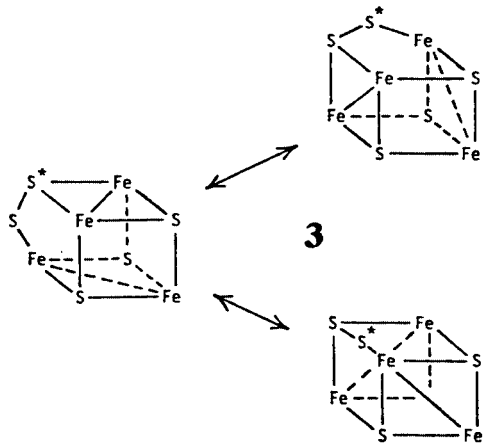

Scheme 7 Reproduced from ref. 23 with permission.

Variable-temperature NMR spectra recorded for **3** and $[\mathbf{3}]^{2+}$ indicated an equivalent environment for three out of the four Fe atoms, which could be explained by the interconversion of the three equivalent structures of Scheme 7, without breaking the S–S bond. Electron-counting considerations and the analogy with $Cp_4Fe_4S_4$ suggest that two metal–metal bonds should be present in **3**, and one more in $[\mathbf{3}]^{2+}$. Kubas and Vergamini noted that the interconversion process portrayed in Scheme 7 implies fluxionality of the metal–metal bonding network, in order to attain the equivalence of the three CpFe moieties.[29]

Similar rearrangements of the metal bonding network were observed and analyzed in detail by Rauchfuss *et al.*[27] At variance with the $Cp_4Fe_4S_5$ cluster, the fluxionality was found in perfect cubane-like $[(RCp)_4Ru_4E_4]^{2+}$ systems (E = S, Se, Te; R = Me, $SiMe_3$), so that it could be assigned *only* to the mobility of the metal–metal bonds associated with intramolecular electron transfer. All the metal atoms in the neutral $Cp_4Ru_4E_4$ clusters are in a similar coordination environment corresponding to the formal oxidation state III (Scheme 8).

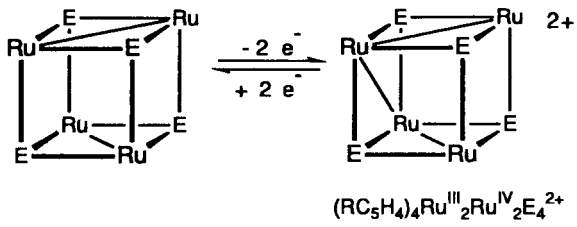

Scheme 8 Reproduced from ref. 27 with permission.

Double oxidation using $MeCpFePF_6$ yields a mixed valence cluster in which two metal atoms have been oxidized into Ru^{IV}. An additional Ru–Ru bond is formed between the Ru^{IV} centers (Scheme 8), distorting the cubane core from idealized T_d to C_2 symmetry, as confirmed by X-ray structures: the three bonded Ru–Ru distances range between 2.78 and 2.81 Å and induce a butterfly folding of the cubic face, in contrast with the three Ru···Ru contacts which average 3.53 Å.

As for $Cp_4Fe_4S_5$, the mobility of the Ru–Ru bonding network was evidenced by the changes observed in the variable-temperature ^{1}H NMR spectra of various $[(RCp)_4Ru_4E_4]^{2+}$ clusters (Fig. 11). At low temperatures (below −30 °C) two

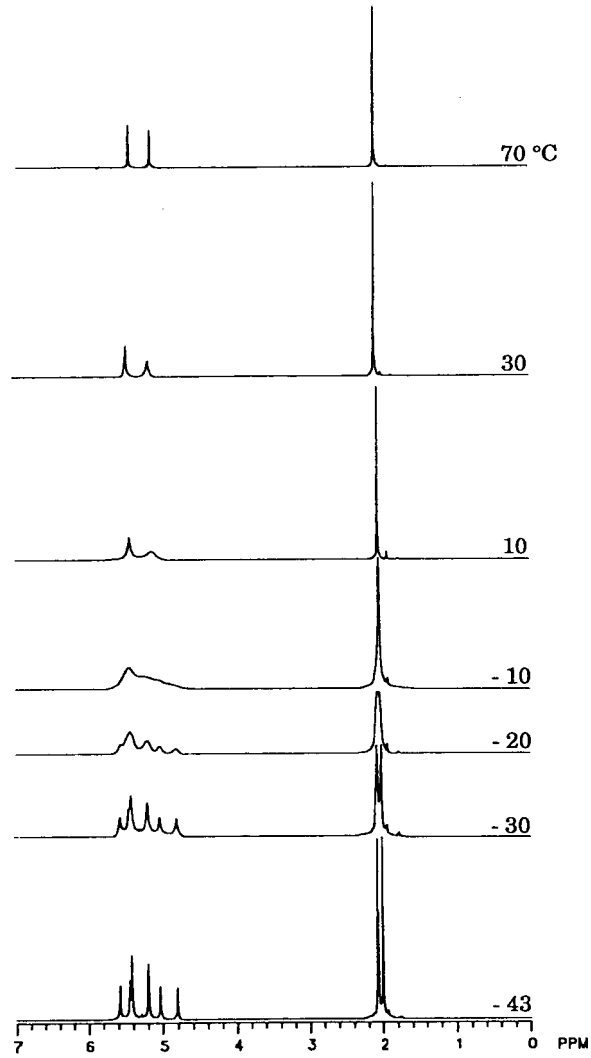

Fig. 11 Variable-temperature 500 MHz ^{1}H NMR spectra of a CD_3CN solution of $(MeC_5H_4)_4Ru_4(PF_6)_2$, obtained by Houser *et al.*[27] Reproduced from ref. 27 with permission.

nonequivalent MeC_5H_4 ligands were observed, as can be seen from both the methyl singlets and the Cp backbone signals. They are assigned to the different coordination spheres of Ru^{III} and Ru^{IV}. The methyl singlets coalesce at about −8 °C, which indicates a free energy barrier of ~52 kJ mol^{-1} to the intramolecular rearrangement.[27]

Other cubane-like structures with mobile metal–metal bonds can be considered. Kabashima *et al.* recently obtained a neutral, mixed-metal cluster with a $TiRu_3S_4$ core from the condensation of two hydrosulfido-bridged dinuclear complexes, $[Cp^*RuCl(\mu_2\text{-}SH)_2RuClCp^*]$ and $[Cp_2Ti(\mu_2\text{-}SH)_2RuClCp^*]$.[30] Application of the effective atomic number (EAN) rule predicts that, with 64 valence electrons, the resulting cluster $[CpTi(Cp^*Ru)_3S_4]$ should display three Ti–Ru and only one Ru–Ru bonds. This was confirmed by the geometrical parameters obtained from X-ray diffraction. The mobility of the Ru–Ru bond between three equivalent positions was established from variable-temperature ^{1}H NMR measurements and the coalescence of the signals at ~0 °C was consistent with an estimate of 55 ± 6 kJ mol^{-1} for the free energy barrier.[30]

Several mechanisms for M–M bond dynamics have been envisioned. However, it should be remembered that the bond migration in $[(RCp)_4Ru_4E_4]^{2+}$ or in $[CpTi(Cp^*Ru)_3S_4]$ cannot generate isomers or conformers since all of the structures formed are identical. The preparation of 'geometric isomers' differing in the basis of their metal–metal bonding network requires the breaking of the structural degeneracy between the various conformations. This was first achieved by grafting on to

the same $[Ru_4E_4]^{2+}$ core different types of cyclopentadienyl ligands, namely C_5H_5, and C_5Me_5 (Cp*).[28] Only one type of crystal structure was characterized, and the $[(Cp)_2(Cp^*)_2Ru_4E_4]^{2+}$ cluster looks quite similar to the parent compound with four identical Cp ligands: a distorted cubane with three bonding Ru–Ru contacts and three nonbonding Ru···Ru distances. However, the three metal–metal bonds are not distributed at random: the Cp*Ru centers each support two metal–metal bonds, suggesting that the corresponding metal atoms can be assigned as Ru^{IV} (Scheme 9, form **4**). The

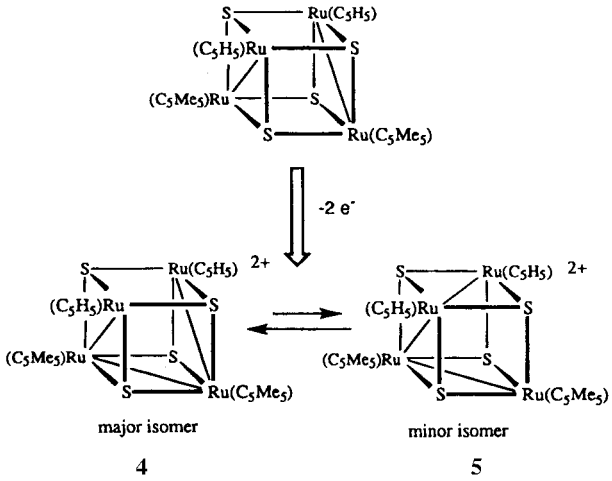

Scheme 9 Reproduced from ref. 28 with permission.

presence of distinct isomers differing in the arrangement of their Ru–Ru bonds could be detected at low temperature in acetone solution, where two ^1H NMR subspectra were detected and assigned to the two structures of Scheme 9. At −90 °C, isomers **4** and **5** are present to the extent of 77 and 23%, respectively.[28]

The metal–metal interactions in $Cp_4M_4X_4$ (M = Mo, Cr, X = S, O) cubane-like clusters have been investigated computationally by McGrady.[31] These clusters contain 12 metal valence electrons and a tetrahedral set of six bonds can be expected to connect all of the metal edges (Scheme 10a). Such a perfect

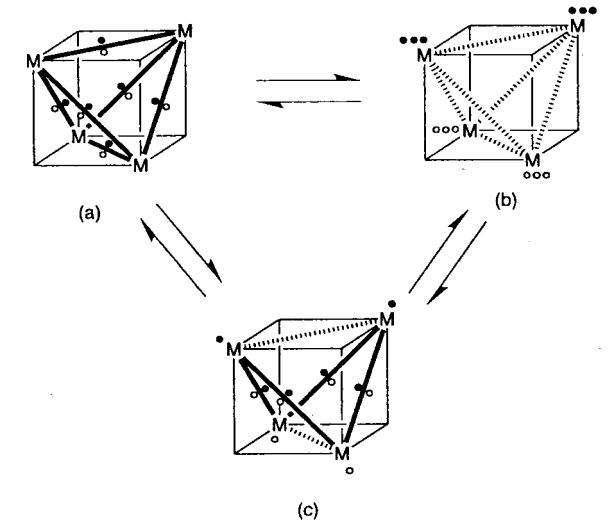

Scheme 10 Reproduced from ref. 31 with permission.

tetrahedral core is effectively observed in $Cp_4M_4S_4$ clusters (M = Mo, Cr) and also in $Cp_4Mo_4O_4$ clusters. Distorted, rhombic structures are however observed for most $Cp_4Cr_4O_4$ clusters and were shown to arise from an antiferromagnetic coupling across four of the six edges of the tetrahedron, and ferromagnetic coupling across the remaining two (Scheme 10b). The electronic configuration with six Cr–Cr bonds corresponds to a low-lying excited singlet state for $Cp_4Cr_4O_4$, and, conversely, the antiferromagnetic coupling becomes the excited state for $Cp_4Cr_4S_4$. The singlet–singlet energy separation is calculated to be of the same order of magnitude ($\sim$11 kcal mol^{-1}) in both cases. The ground state of the molybdenum clusters, $Cp_4Mo_4S_4$ and $Cp_4Mo_4O_4$ is very similar to that of $Cp_4Cr_4S_4$, characterized by a tetrahedral core and 6 M–M bonds. However, the Mo clusters exhibit a different type of excited state, corresponding to the covalent bonding of eight electrons, whereas the four leftover electrons remain localized on the Mo centers and give rise to two antiferromagnetic couplings (Scheme 10c). The structural consequence is a very strong rhombic distortion of the cuboidal framework.[31] It would be of interest to investigate, both experimentally and computationally, mixed-metal complexes of the type $Cp_4Mo_2Cr_2O_4$ which might exhibit a double well on the singlet ground-state potential energy surface.

4.3 Intramolecular electron transfer in functionalized polyoxometalates

The breaking of a metal–metal bond through an intramolecular redox process can finally be achieved without concerted formation of another bond if the electron pair is transferred to a molecular fragment capable of accommodating these electrons without too much deformation of the nuclear framework. This implies the availability of empty, nonbonding or weakly bonding orbitals in the fragment to be reduced. Such electron reservoirs are well documented in the fullerene family. Most polyoxometalate cluster anions, made of highly oxidized metals of groups 5 or 6 in an octahedral environment of oxygen atoms, can also undergo several facile reduction steps without displaying noticeable structural deformation. The additional electrons are accommodated in metal orbitals just slightly stabilized by π donation from the oxo ligands. The question of the localization, or delocalization over the metal framework of the so-called 'blue electrons'—because of the characteristic color of the reduced polyoxometalate species—is still a debated problem.[32]

We have recently assessed, by means of DFT calculations, the first case of an intramolecular redox process between a metal–metal bond and a polyoxometalate core.[33] The systems we investigated consist of a series of four heteropolyanions synthesized by Cadot *et al*. through stereospecific addition of the dications $[M^V_2X_2O_2]^{2+}$ (M = Mo^V, W^V; X = O, S) to the divacant $[SiW^{VI}_{10}O_{38}]^{8-}$ anion in dimethylformamide.[34] The two oxothio anions could be isolated in crystal form and structurally characterized (Fig. 12; Table S4, ESI). This type of

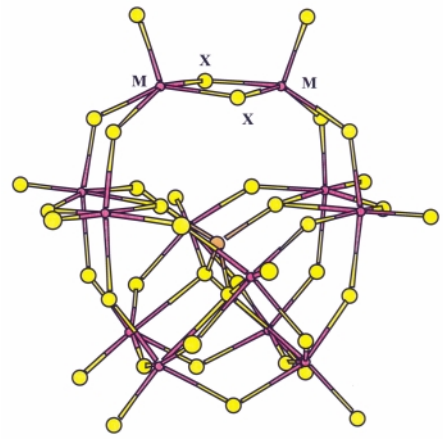

Fig. 12 XMOL view of γ-$[SiW_{10}M_2X_2O_{38}]^{6-}$ (M = Mo, W; X = S, O) in the conformation corresponding to a short M–M distance. Unlabeled atoms are as follows: Si (orange); W (pink); oxygen (yellow).

cluster organization is referred to as γ-Keggin according to the structural classification of polyoxometalates. The coordination geometry about the M^V atoms is that of two square pyramids

sharing a common basal edge formed by the two sulfur atoms. A short M^V–M^V separation is observed for γ-$[SiW_{10}Mo_2S_2O_{38}]^{6-}$ (**6**; Mo–Mo = 2.832 Å) as for $[SiW_{12}S_2O_{38}]^{6-}$ (**7**; W–W = 2.815 Å). These distances are clearly indicative of a metal–metal single bond.[34] The oxo anions $[SiW_{10}Mo_2O_{40}]^{6-}$ (**8**) and $[SiW_{12}O_{40}]^{6-}$ (**9**) could not be characterized crystallographically. It appeared however that the dodecatungsten oxoanion **9** could be different from the three other clusters. More specifically, the blue color of the solution and solid residues containing **9** contrasts with the red or red–brown appearance of the equivalent material obtained with **6**, **7**, and **8** and suggests a reduction of the polyoxometalate core.

Geometry optimization of the four clusters was carried out by means of DFT calculations, starting either from the experimental structure, when available, or from equivalent geometries with short M^V–M^V distances. At the end of the optimization process, all four systems displayed qualitatively similar electronic structures, with an occupied oxygen–sulfur valence band, a high-lying, empty metal d band and an isolated HOMO characteristic of the metal–metal σ bond in the $M_2X_2O_2$ fragment (Fig. 13). The M^V–M^V distances calculated at equilibrium were in keeping with the presence of a metal–metal bond.

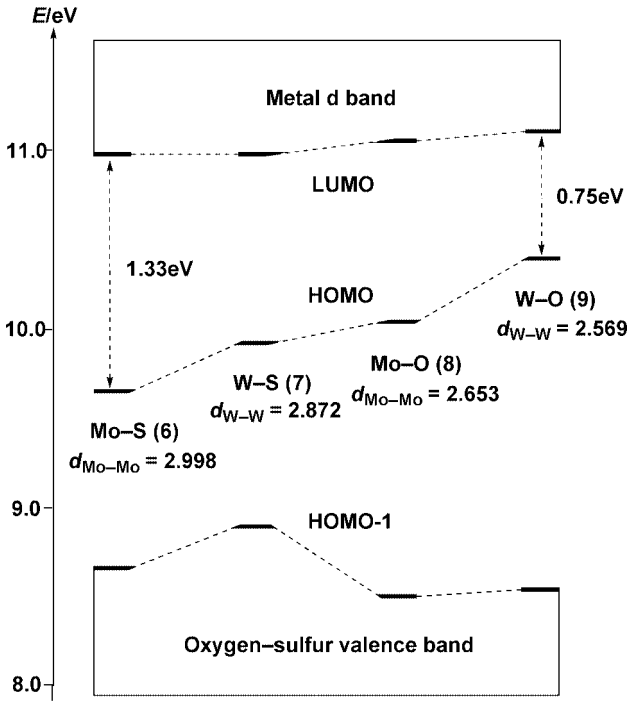

Fig. 13 Energies of the Kohn–Sham frontier orbitals calculated for γ-$[SiW_{10}M_2X_2O_{38}]^{6-}$ (M = Mo, W; X = S, O) at the equilibrium geometry associated with a single M–M bond.

As shown in Fig. 13, the energy of the metal–metal bonding HOMO is not constant in the series of clusters: this orbital is increasingly destabilized as the metal–metal bond becomes shorter. This can be explained quite easily: the metal–metal bonding HOMO is also the *metal–ligand* antibonding counterpart of a low-energy, all-bonding MO with major weight on the ligand p orbitals directed toward the center of the M_2X_2 core (Scheme 11).

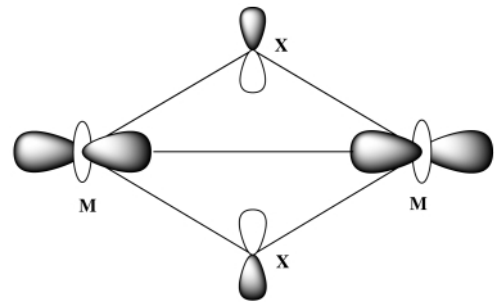

Scheme 11

A contraction of the metal–metal distance increases the metal–ligand overlap and the strength of the metal–ligand interaction. The antibonding term of this interaction is therefore pushed to higher energies (Fig. 13). Such a four-electron interaction is known to be globally unfavorable. When the contraction of the M_2X_2 core pushes the HOMO close enough to the empty d band, it could become advantageous to delocalize the electrons over the γ-Keggin tungsten framework, *even at the expense of the M–M bond.*

Another series of calculations was therefore carried out starting from trial structures of **6**, **7**, **8** and **9** in which the M–M distance had been overstretched. For all of the clusters, the bridged dimetal fragment evolved toward a new equilibrium conformation characterized by a long M–M distance (Table S4). Compared with the previous equilibrium conformation, the electronic structure of the new state is characterized by a level crossing between the former HOMO, with M–M bonding character (Fig. 14 left) and the lowest orbital of the metal d band, widely delocalized over the metal framework of the Keggin ion (Fig. 14 right).

In the singular case of $[SiW_{12}O_{40}]^{6-}$ (**9**), the new, delocalized (D) state is lower in energy by 0.13 eV (2.9 kcal mol^{-1}) (Fig. 15).[33] For clusters **6**, **7** and **8**, the state with a localized metal–metal bond (L state) is energetically preferred by more than 10 kcal mol^{-1}.

A DFT estimate of the energy associated with the transition state separating the two conformations showed that the highest barrier (5.6–5.8 kcal mol^{-1}) is obtained for **9**. This is clearly not sufficient to make a physical separation of the two conformers possible at room temperature. The very close energy values obtained for both conformations suggest that they should coexist in solution. Further studies are in progress to obtain a structural characterization of **9** and to enhance the value of the barrier through an appropriate tuning of the dimetal cationic moiety.

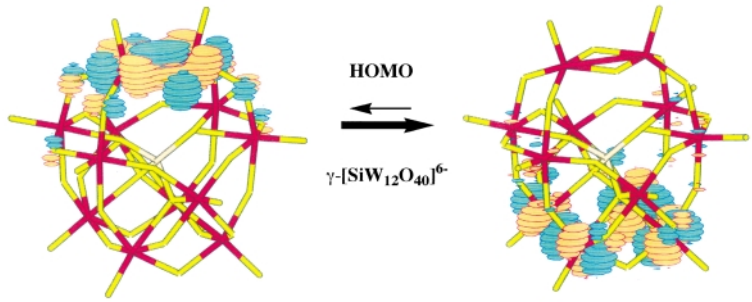

Fig. 14 Graphical representation of the HOMO for the two energy minima characterized from DFT/BP86 calculations on the singlet ground-state potential energy surface of γ-$[SiW_{12}O_{40}]^{6-}$. Left: conformation associated with an M–M σ bond; right: conformation associated with the distribution of the metal electrons delocalized over the Keggin core.

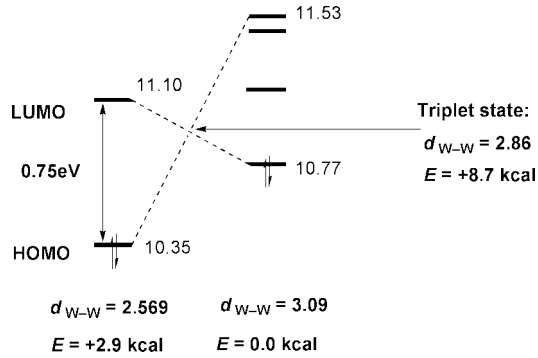

Fig. 15 $[SiW_{12}O_{40}]^{6-}$: schematic representation of the energy crossing occurring between the HOMO (a_1 symmetry) and the LUMO (a_2 symmetry) along the displacement coordinate connecting the two minima of the potential energy surface. The position and the relative energy of the crossing point have been estimated from an optimization of the lowest triplet state. Orbital energies in eV; relative state energies in kcal mol^{-1}.

5 Structural variability of the linear metal frameworks $(Co_3)^{6+}$ and $(Cr_3)^{6+}$

5.1 Structural investigations on $M_3(dpa)_4Cl_2$ (M = Co, Cr), $Co_3(dpa)_4(Cl)L'$ (L′ = BF_4, PF_6) and related compounds

The dipyridylamide anion (dpa) is a tridentate ligand, appreciably bent because of steric repulsion between two hydrogens, which has been used to stabilize a number of neutral or charged complexes built around a framework of three transition metal atoms in a linear conformation. Complexes of the type $M_3(dpa)_4L_2$ or $M_3(dpa)_4LL'$ are known, with M = Cr, Co, Ni, Cu, Ru, Rh. The axial ligands may be either halogen atoms or molecular anions. In the five past years, Cotton and co-workers have thoroughly investigated these compounds and shown that the cobalt and the chromium complexes belonging to this family share a structural variability affecting primarily the metal framework and which seems unprecedented in coordination chemistry.[35–37] The most extensively documented case concerns $Co_3(dpa)_4Cl_2$, which is able to exist with either a symmetrical (*s*) Co_3 chain or an unsymmetrical (*u*) one, depending only on the crystal form in which it is found (Scheme 12, Fig. 16).[35,36]

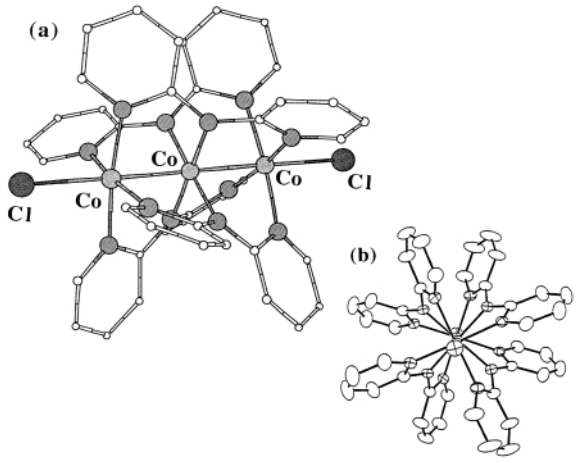

Fig. 16 Schematic representations of $Co_3(dpa)_4Cl_2$: (a) perspective view; (b) a view looking down the Co_3 axis.

This behavior is obviously reminiscent of bond-stretch isomerism. The temperature dependence of the structural parameters is also extremely unusual. In the *s* form, both Co–Co bond lengths are of the order of 2.31 Å at 110 or 120 K, but a stretching of the metal–metal bonds has been observed in some cases as the temperature increases to room temperature. This

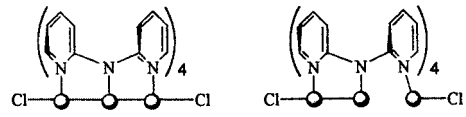

***s*-$Co_3(dpa)_4Cl_2$** ***u*-$Co_3(dpa)_4Cl_2$**

Scheme 12 Reproduced from ref. 35 with permission.

stretching may be important (0.043 Å for $Co_3(dpa)_4Cl_2{\cdot}C_6H_{12}$; 0.064 Å for $Co_3(dpa)_4Br_2{\cdot}C_6H_{12}$) but the structure remains basically symmetric. In the *u* form, the Co–Co bond lengths are typically 2.46–2.50 Å ('long bond') and around 2.28 Å ('short bond') at room temperature. However, the whole structural environment of the terminal Co atom taking part in the long Co–Co bond, including the Co–N bond lengths, is strongly affected by temperature changes. The long Co–Co bond itself contracts by 0.086 Å between 298 and 20 K and the complex becomes 'less unsymmetrical' at low temperature.[36] Magnetic susceptibility measurements have shown that both the *s* and the *u* isomers are in an $S = ½$ ground state at low temperature, but exhibit gradual spin crossover at higher temperature.[35]

As noted above, structural variability also affects the trinuclear complexes of chromium, $Cr_3(dpa)_4L_2$ and $Cr_3(dpa)_4LL'$, but in a somewhat different way. Complexes with identical axial ligands such as L = Cl or phenylacetylene exhibit metal frameworks that are either symmetric or slightly unsymmetrical (Table S6, ESI). However, if one axial ligand is replaced by a weak σ-donor, such as BF_4^- or PF_6^-, the metal framework adopts an extremely distorted structure characterized by a 'supershort' Cr–Cr bond of ~2.0 Å with the third metal atom at a distance of more than 2.6 Å. No such conformation has been characterized for neutral $Cr_3(dpa)_4Cl_2$ and the metal–metal separations observed in $Cr_3(dpa)_4L_2$ and in $Cr_3(dpa)_4LL'$ clearly correspond to different categories, even though the magnetic behavior of both structural types is consistent with a quintet ground state ($S = 2$).[37]

The abundant structural documentation presently available on $M_3(dpa)_4L_2$ and $M_3(dpa)_4LL'$ complexes raises at least two puzzling questions. (i) How can the similarities observed in the structural behavior of the complexes of chromium and cobalt be explained, in spite of their different electron count and magnetic behavior? (ii) Is the structural variability found for $Co_3(dpa)_4Cl_2$ and still under investigation for $Cr_3(dpa)_4L_2$ and $Cr_3(dpa)_4LL'$ compounds relevant to Parkin's definition of bond-stretch isomerism? It seems that theoretical investigations can shed some light on both problems.

5.2 Are $Co_3(dpa)_4Cl_2$ and $Cr_3(dpa)_4Cl_2$ electronically similar to the allyl radical?

Spin-unrestricted DFT calculations carried out on $Co_3(dpa)_4Cl_2$ confirm that the molecular ground state is low spin ($S = ½$). In agreement with standard electron counting, the $(Co_3)^{6+}$ framework accommodates 21 metal electrons. In a linear triatomic system, the equivalent atomic orbitals of every type give rise to a set of three molecular orbital (MO) combinations: (i) a bonding MO, lowest in energy, (ii) a nonbonding one, antisymmetric and localized on the terminal atoms, and (iii) an antibonding MO. The d orbitals of transition metals generate five such sets: one σ set, composed of d_{z^2} orbital combinations (*z* is collinear with the framework axis); two degenerate π sets, combinations of d_{xz} and d_{yz} orbitals; and two δ sets, combinations of d_{xy} and $d_{x^2-y^2}$ orbitals. The orbitals of one δ set face the lone pairs of the equatorial dpa ligands and play the role of acceptor orbitals in the donation interactions.

The 3d atomic orbitals are rather compact in space and the 3d–3d overlap between π and, even more so, between δ orbitals is weak except at supershort distances. The nine metal MOs belonging to the two π sets and to the remaining δ set are not

significantly split in energy. Eighteen out of the 21 metal electrons are accommodated in this block of 9 MO combinations, which are therefore completely occupied. The splitting is more important between the three orbitals of the σ set: the σ-bonding MO lies below the π/δ block and is doubly occupied, whereas the σ-nonbonding MO is just *above* the π/δ block and accommodates the unpaired electron (Fig. 17). *In the symmetric conformation*, the σ-antibonding MO represents the LUMO, separated from the singly occupied orbital by an energy gap of ~1.1 eV.

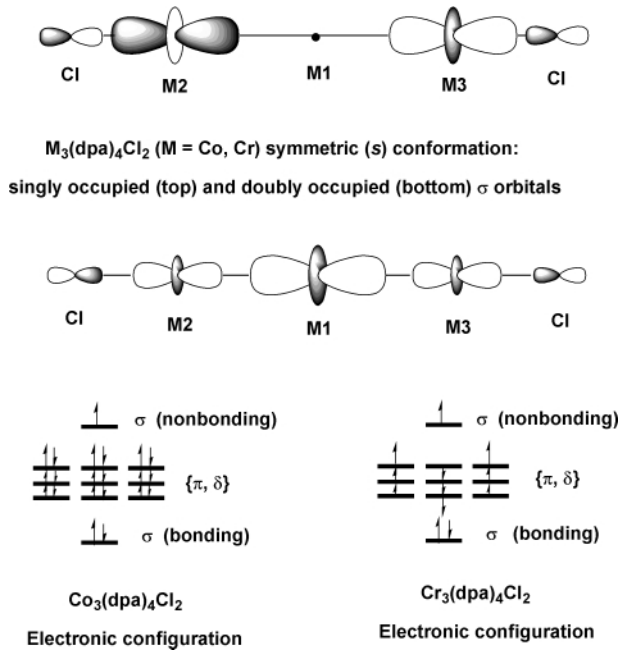

Fig. 17 $M_3(dpa)_4Cl_2$ (M = Co, Cr); symmetric form: sequence of the metal orbitals and their occupancies. Scheme of the doubly occupied, σ-bonding MO and of the singly occupied, σ-nonbonding MO.

The 18 electrons accommodated in the π and δ orbital sets do not take part in any metal–metal interaction, either bonding, or antibonding. They can be considered as *localized* on individual metal atoms. The bonding in the metal framework is therefore exclusively due to the three σ electrons, which are *delocalized* over the metal framework. As for the π system of the allyl radical and for the valence orbitals of alkali or coinage metal trimers, the σ orbital set of $Co_3(dpa)_4Cl_2$ provides a typical example of three-electron, three-center system.[38]

Rather unexpectedly, the electronic structure of $Cr_3(dpa)_4Cl_2$ happens to be very similar to that of the cobalt complex. The sequence of the twelve d orbitals mirrors that of the cobalt system, but the electron count of the $(Cr_3)^{6+}$ framework is 12 electrons only. In the symmetric form, however, all the nine orbitals of the π/δ block are again equally occupied, *but with one electron each*. As for the tricobalt complex, the three remaining electrons are accommodated in the σ set, so as to achieve a delocalized three-electron, three-center bond. As for the cobalt complex, there is no net covalent bonding originating from the π and δ orbitals. At variance with $Co_3(dpa)_4Cl_2$, however, the 10 unpaired electrons—including the electron accommodated in the σ nonbonding orbital and shared between the terminal Cr atoms—are *spin-coupled*. The coupling corresponds to an antiferromagnetic interaction between 3 electrons with β spin, localized on the central Cr atom, and 7 electrons with α spin positioned on both ends of the metallic framework.

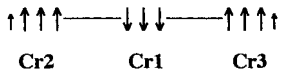

The spin densities assigned to the metal atoms in the optimal, symmetric conformation (+3.52, −3.00, +3.52, ascribing a negative sign to the electrons with β spin) exactly conform to this coupling scheme. The resulting spin therefore corresponds to $S = 2$, in agreement with the magnetic measurements. In order to estimate the energy associated with the antiferromagnetic spin coupling, a single point calculation has been carried out at the optimal geometry, compelling the ten unpaired electrons to have parallel spins. The resulting state ($S = 5$) is destabilized by 30.8 kcal mol^{-1} (Fig. 18, 'green' coupling).

Structure	S value	Spin Coupling Atomic Spin Populations	Relative Energies
Symmetric $\Delta d_{Cr\text{-}Cr} = 0$	2	↑↑↑↑ —— ↓↓↓ —— ↑↑↑↑ 3.52 -3.00 3.52	0.0
Non-symmetric $\Delta d_{Cr\text{-}Cr} = 0.106$	2	↑↑↑↑ —— ↓↓↓ —— ↑↑↑↑ 3.60 −3.00 3.44	+0.97
Non-symmetric $\Delta d_{Cr\text{-}Cr} = 0.679$	2	↑↑↑↑ ---- ↓↓↓ ≡≡ ↑↑↑ 3.79 −2.27 2.50	+4.25
Non-symmetric $\Delta d_{Cr\text{-}Cr} = 0.679$	2	↑↑↑↑ ---- ↑↑↑ ≡≡ ↓↓↓ 3.84 2.17 −2.09	+10.12
Symmetric $\Delta d_{Cr\text{-}Cr} = 0$	5	↑↑↑↑ —— ↑↑↑ —— ↑↑↑↑ 3.50 2.93 3.50	+30.8

Fig. 18 Spin-coupling scheme, atomic spin populations and relative energies (kcal mol^{-1}) for various electronic configurations (represented by different colours) calculated for the symmetric form ($\Delta d_{Cr–Cr} = 0$); for a slightly distorted form ($\Delta d_{Cr–Cr} = 0.106$ Å) and for the highly distorted structure ($\Delta d_{Cr–Cr} = 0.679$ Å).

5.3 $M_3(dpa)_4Cl_2$ (M = Co, Cr): electronic origin of the structural versatility

The similarities and differences in the structural behavior of the linear trimetallic complexes of cobalt and chromium can be interpreted in terms of their electronic structure. It first appears that both types of complexes display a ground-state potential energy curve with a shallow minimum, corresponding to the *s* conformation. Both the shape of this PES and the symmetric position of its minimum are consequences of the three-electron, three-center bond, which is quite similar for cobalt and for chromium. The shallowness of the potential curve had already been noticed for classical three-electron, three-center systems like Cu_3, alkali trimers, or the allyl radical. For $Co_3(dpa)_4Cl_2$, a difference of 0.085 Å between the two Co–Co bond lengths similar to what is observed for the *u* form at 20 K destabilizes the complex by no more than 1.1 kcal mol^{-1}. How could the structural characterization of the *u* form then be explained? No second minimum was found on the doublet ground-state PES of the isolated molecule, ruling out the hypothesis of bond-stretch isomerism. The shallowness of the PES suggested that the crystal forces could influence the molecular geometry, but modelling the application of a strong electric field collinear with the framework axis had no real effect on stabilizing the distorted conformation. It appears, in agreement with the result of magnetic measurements, that spin crossover should be responsible for the structural variability with respect either to the crystal environment or to the temperature.[38]

The same type of shallow, symmetric PES governed by σ metal electrons was calculated for $Cr_3(dpa)_4L_2$. At variance with the cobalt complex however, the underlying π and δ electrons, though localized on the metal atoms, are not inactive and take part in the bonding through their magnetic coupling. In the symmetric ground state, the coupling (represented in blue in Fig. 18) is antiferromagnetic between the 3 electrons localized

on the central chromium and the 7 unpaired electrons including the σ nonbonding electron, accommodated on the terminal metal atoms. The potential energy curve with respect to the framework distortion closely parallels that of $Co_3(dpa)_4Cl_2$. A slight distortion analogous to that observed in compound **12** of Table S6 (Δd_{Cr-Cr} = 0.106 Å) destabilizes the isolated $Co_3(dpa)_4Cl_2$ complex by less than 1 kcal mol^{-1} (Fig. 18). If the Cr–Cr distances are constrained to differ by 0.67 Å so as to reproduce the framework geometries observed for $Co_3(dpa)_4$-(Cl)L′ (L′ = BF_4, PF_6), then the destabilisation does not exceed 4.25 kcal mol^{-1} (Fig. 18). In this conformation, the antiferromagnetic coupling between the 9 π and δ electrons remains basically similar, namely ↑ ↑ ↑ ··· ↓ ↓ ↓ — ↑ ↑ ↑ but the coupling along the 'supershort' metal–metal distance evolves toward a multiple bond with covalent character.[39] For such a highly unsymmetrical structure, however, another type of spin coupling is characterized between the 9 non-σ electrons: still antiferromagnetic-like along the supershort Cr–Cr bond, the coupling is *ferromagnetic* between the nonbonded metal atoms (Fig. 18, 'red' coupling). This new electronic configuration,

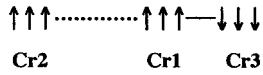

also corresponding to a quintet spin state, gives rise to a stable minimum of the strongly unsymmetrical conformation. For $Cr_3(dpa)_4Cl_2$, the relative energy associated with the distorted equilibrium conformation is +10.1 kcal mol^{-1} with respect to the symmetric ground state, and, still +5.9 kcal mol^{-1} with respect to the energy of the ground state electronic conformation *calculated at the distorted geometry*. These results show that there is only one minimum on the quintet ground-state PES *of* $Cr_3(dpa)_4Cl_2$, which appears to be in agreement with experimental observation. They also suggest that a second spin coupling scheme, inherently associated with a highly distorted structure, could be stabilized by an unsymmetrical arrangement of the axial ligands. We therefore predict that a convenient tuning of axial coordination should give rise to separate energy minima on the quintet ground-state potential energy surface and therefore generate real bond-stretch isomers, with a $(Cr_3)^{6+}$ metal framework either symmetric, or highly nonsymmetric.[39] Calculations on real and hypothetical $Cr_3(dpa)_4LL'$ compounds are in progress to check this hypothesis.

6 Miscellaneous

Some rare cases of isomerism have been characterized in transition metal chemistry that affect the geometry of the metal core. In that sense, this 'core isomerism'[40] seems reminiscent of the geometric isomerism characterized in cubane-like M_4S_4 clusters (Section 4.2). At variance with this case, however, the conformational change does not originate in the electronic structure of the core itself, but rather involves a balance between the stabilization offered by a metal–metal bond, on the one hand, or by the enhancement of a favorable interaction with a strong σ-donor ligand, on the other. The most classical example concerns the $Pt_3(\mu\text{-}PPh_2)_4Ph(PPh_3)_2$ cluster,[40] in which the triangular metal core can either be close to threefold symmetry (Pt–Pt = 2.956, 2.956 and 3.074 Å), or display two short and one long bonds (Pt–Pt = 2.758, 2.758 and 3.586 Å), the stretched Pt–Pt bond being opposite the Ph ligand. The intricate relationship between the metal–metal and the metal–ligand interactions has been rationalized by means of extended Hückel calculations.[40]

The origin of the isomerism affecting the Ru–Ru bond length in $(Cp^*RuCl)_2(\mu\text{-}Cl)_2$ is more controversial. The elongation of the metal–metal distance from 2.930 to 3.752 Å was assigned to a change in the spin coupling between the Ru atoms from antiferromagnetic (singlet spin state) in the short-bonded conformation to ferromagnetic (triplet spin state) in the long-bonded one. These species were therefore termed 'spin-state' rather than 'bond-stretch' isomers.[41] Recent DFT calculations by McGrady, however, suggest that a second energy minimum should also appear at a long Ru–Ru distance on the PES of the *singlet* spin state.[42]

7 Conclusions

Bond-stretch isomerism has had a complicated history. Approximately at the same time, it was independently introduced as a theoretical concept,[4] and demonstrated in some molybdenum oxo complexes as an achievement of crystallography, which was later revealed to be an artifact of crystallography.[5] When the myth of the two Mo–O distances in $MoOCl_2(PR_3)_3$ complexes and other 'bogus isomers'[43] collapsed in the early nineties, Parkin wrote in the conclusion of his review that 'although the original example of bond-stretch isomerism has been shown to be the result of an artifact and that there is presently no definitive evidence of bond-stretch isomerism in other complexes, the concept itself still remains. Only a combination of time and a demanding series of analytical experiments will reveal whether or not if it is actually possible for bond-stretch isomers to exist under normal conditions'.[5] Almost a decade after this statement, the experiments have been carried out and have characterized rare, but doubtless cases of BSI, some of the most remarkable examples being the X-ray characterization of the monocyclic and bicyclic forms of $[(Mes^*P)_2CHCSiMe_3]$,[20] the evidence for a reversible cleavage of the O–O bond in synthetic analogs of oxyhemocyanin,[26] and the substantiation of a 'geometric isomerism' in cubane-like M_4S_4 clusters by means of variable-temperature ^{1}H NMR spectroscopy.[28] Beyond the characterization of real isomers or conformers, a growing corpus of studies concludes that BSI has not yet been proven, but should potentially exist with a proper tuning of the substituents or ligands. Let us mention again the monocyclic or bicyclic forms of the M_4R_6 species (M = Si, Ge, Sn, Pb), some edge-sharing dimers of transition metals, functionalized polyoxometalates, and the complexes formed around a linear chain of chromium atoms. Most of these studies are based on, or at least include, a theoretical part which proves the relevance of the BSI concept through the characterization of a double well, associated with the same spin multiplicity, on the ground-state potential energy surface of an isolated molecule. This criterion was already stressed in the original studies by Stohrer and Hoffmann of strained hydrocarbons and related molecules.[4] It could be however convenient to complete Parkin's purely phenomenological definition with another interpretation of bond-stretch isomers (or conformers) in which they are viewed as molecules that retain in the gas phase distinct ground-state equilibrium positions, either stable or metastable, along a reaction pathway defined by the stretching of a bond.

8 Acknowledgments

Calculations on $[SiW_{12}O_{40}]^{6-}$, on related polyoxometalate compounds and on $M_3(dpa)_4Cl_2$ (M = Co, Cr) have been carried out in part at the Centre Universitaire et Régional de Ressources Informatiques (CURRI, Université Louis Pasteur, Strasbourg, France) and in part at the IDRIS computer center (CNRS, Orsay, France). We are pleased to thank Professor F. A. Cotton and C. A. Murillo for stimulating discussions and for communicating their most recent results and structures. The

work on $Cr_3(dpa)_4Cl_2$ was initiated by Mr Noureddine Benbellat during his undergraduate research period.

9 References

1 A. Joly, *Cours élémentaire de Chimie, Chimie générale—Métalloïdes*, Librairie Hachette, Paris, 1894, p. 36.
2 Y. Jean, A. Lledos, J. K. Burdett and R. Hoffmann, *J. Am. Chem. Soc.*, 1988, **110**, 4506.
3 H. Jacobsen, H. W. Schmalle, A. Messmer and H. Berke, *Inorg. Chim. Acta*, 2000, **306**, 153.
4 W. D. Stohrer and R. Hoffmann, *J. Am. Chem. Soc.*, 1972, **94**, 779.
5 G. Parkin, *Chem. Rev.*, 1993, **93**, 887.
6 S. M. Casey and D. G. Leopold, *J. Phys. Chem.*, 1993, **97**, 816; and references cited therein.
7 H. Dachsel, R. J. Harrison and D. A. Dixon, *J. Phys. Chem. A*, 1999, **103**, 152; and references cited therein.
8 N. A. Baykara, B. N. McMaster and D. R. Salahub, *Mol. Phys.*, 1984, **52**, 891.
9 M. M. Goodgame and W. A. Goddard III, *Phys. Rev. Lett.*, 1985, **54**, 661.
10 M. Moskovits, W. Limm and T. Mejean, *J. Chem. Phys.*, 1985, **82**, 4875.
11 H. Stoll and H.-J. Werner, *Mol. Phys.*, 1996, **88**, 793.
12 B. O. Roos, *Acc. Chem. Res.*, 1999, **32**, 137.
13 K. E. Edgecombe and A. D. Becke, *Chem. Phys. Lett.*, 1995, **244**, 427.
14 E. R. Davidson, *Chem. Phys. Lett.*, 1998, **284**, 301; and references cited therein.
15 S. Nagase, *Acc. Chem. Res.*, 1995, **28**, 469; and references cited therein.
16 G. Trinquier and C. Jouany, *J. Phys. Chem. A*, 1999, **103**, 4723.
17 P. v. R. Schleyer, A. F. Sax, J. Kalcher and R. Janoschek, *Angew. Chem., Int. Ed. Engl.*, 1987, **26**, 364.
18 J. A. Boatz and M. S. Gordon, *J. Phys. Chem.*, 1989, **93**, 2888.
19 F. Zürcher and R. Nesper, *Angew. Chem., Int. Ed.*, 1998, **37**, 3314.
20 E. Niecke, A. Fuchs and M. Nieger, *Angew. Chem., Int. Ed.*, 1999, **38**, 3028; and ref. 3 therein.
21 J. M. Schulman and R. L. Disch, *J. Am. Chem. Soc.*, 1993, **115**, 11153.
22 R. Boese, J. Benet-Buchholz, A. Stanger, K. Tanaka and F. Toda, *Chem. Commun.*, 1999, 319.
23 S. Alvarez, A. A. Palacios and G. Aullón, *Coord. Chem. Rev.*, 1999, **185–186**, 431; and references cited therein.
24 (*a*) C. Mealli and D. M. Proserpio, *J. Am. Chem. Soc.*, 1990, **112**, 5484; (*b*) C. Mealli and A. Orlandini, *Metal Clusters in Chemistry*, eds. P. Braunstein, L. A. Oro and P. R. Raithby, Wiley-VCH, Weinheim, 1999, vol. 1, pp. 143–162.
25 A. A. Palacios, G. Aullón, P. Alemany and S. Alvarez, *Inorg. Chem.*, 2000, **39**, 3166.
26 J. A. Halfen, S. Mahapatra, E. C. Wilkinson, S. Kaderli, V. G. Young Jr., L. Que Jr., A. D. Zuberbühler and W. B. Tolman, *Science*, 1996, **271**, 1397.
27 E. J. Houser, T. B. Rauchfuss and S. R. Wilson, *Inorg. Chem.*, 1993, **32**, 4069.
28 Q. Feng, T. B. Rauchfuss and S. R. Wilson, *J. Am. Chem. Soc.*, 1995, **117**, 4702.
29 G. J. Kubas and P. J. Vergamini, *Inorg. Chem.*, 1981, **20**, 2667.
30 S. Kabashima, S. Kuwata, K. Ueno, M. Shiro and M. Hidai, *Angew. Chem., Int. Ed.*, 2000, **39**, 1128.
31 J. E. McGrady, *J. Chem. Soc., Dalton Trans.*, 1999, 1393.
32 J.-M. Maestre, J.-M. Poblet, C. Bo, N. Casan-Pastor and P. Gomez-Romero, *Inorg. Chem.*, 1998, **37**, 3444.
33 M.-M. Rohmer, M. Bénard, E. Cadot and F. Sécheresse, *Polyoxometalate Chemistry: From Topology* via *Self-Assembly to Applications*, eds. M. T. Pope and A. Müller, Kluwer Academic, Dordrecht, The Netherlands, 2001, pp. 117–133.
34 E. Cadot, V. Béreau, B. Marg, S. Halut and F. Sécheresse, *Inorg. Chem.*, 1996, **35**, 3099.
35 R. Clérac, F. A. Cotton, L. M. Daniels, K. R. Dunbar, C. A. Murillo and X. Wang, *Inorg. Chem.*, 2001, **40**, 1256; and references cited therein.
36 R. Clérac, F. A. Cotton, L. M. Daniels, K. R. Dunbar, K. Kirschbaum, C. A. Murillo, A. A. Pinkerton, A. J. Schultz and X. Wang, *J. Am. Chem. Soc.*, 2000, **122**, 6226.
37 R. Clérac, F. A. Cotton, L. M. Daniels, K. R. Dunbar, C. A. Murillo and I. Pascual, *Inorg. Chem.*, 2000, **39**, 748.
38 M.-M. Rohmer, A. Strich, M. Bénard and J.-P. Malrieu, *J. Am. Chem. Soc.*, 2001, **123**, 9126.
39 N. Benbellat, M.-M. Rohmer and M. Bénard, *Chem. Commun.*, in the press.
40 R. Bender, P. Braunstein, A. Dedieu, P. D. Ellis, B. Huggins, P. D. Harvey, E. Sappa and A. Tirippicchio, *Inorg. Chem.*, 1996, **35**, 1223.
41 G. Parkin and R. Hoffmann, *Angew. Chem., Int. Ed. Engl.*, 1994, **33**, 1462.
42 J. E. McGrady, *Angew. Chem., Int. Ed.*, 2000, **39**, 3077.
43 F. A. Cotton, M. Kohli, R. L. Luck and J. V. Silverton, *Inorg. Chem.*, 1993, **32**, 1868.